ORIGINAL PAPER

Transient Spark Discharge Generated in Various N_2/O_2 Gas Mixtures: Reactive Species in the Gas and Water and Their Antibacterial Effects

Katarína Kučerová[1] · Zdenko Machala[1] · Karol Hensel[1]

Abstract

Reactive species generated in the gas and in water by cold air plasma of the transient spark discharge in various N_2/O_2 gas mixtures (including pure N_2 and pure O_2) have been examined. The discharge was operated without/with circulated water driven down the inclined grounded electrode. Without water, NO and NO_2 are typically produced with maximum concentrations at 50% O_2. N_2O was also present for low O_2 contents (up to 20%), while O_3 was generated only in pure O_2. With water, gaseous NO and NO_2 concentrations were lower, N_2O was completely suppressed and HNO_2 increased; and O_3 was lowered in O_2 gas. All species production decreased with the gas flow rate increasing from 0.5 to 2.2 L/min. Liquid phase species (H_2O_2, NO_2^-, NO_3^-, ·OH) were detected in plasma treated water. H_2O_2 reached the highest concentrations in pure N_2 and O_2. On the other hand, nitrites NO_2^- and nitrates NO_3^- peaked between 20 and 80% O_2 and were associated with pH reduction. The concentrations of all species increased with the plasma treatment time. Aqueous ·OH radicals were analyzed by terephthalic acid fluorescence and their concentration correlated with H_2O_2. The antibacterial efficacy of the transient spark on bacteria in water increased with water treatment time and was found the strongest in the air-like mixture thanks to the peroxynitrite formation. Yet, significant antibacterial effects were found even in pure N_2 and in pure O_2 most likely due to high ·OH radical concentrations. Controlling the N_2/O_2 ratio in the gas mixture, gas flow rate, and water treatment time enables tuning the antibacterial efficacy.

Keywords Cold atmospheric plasma · Plasma activated water · N_2/O_2 gas mixture · Antibacterial effects · Reactive oxygen and nitrogen species

✉ Zdenko Machala
  machala@fmph.uniba.sk

  Katarína Kučerová
  tarabovakatarina@gmail.com

[1] Division of Environmental Physics, Faculty of Mathematics, Physics and Informatics, Comenius University, Mlynská dolina, 84248 Bratislava, Slovakia

⧉ Springer

Introduction

Cold atmospheric plasmas, also known as low-temperature, non-thermal or non-equilibrium plasmas have been widely studied in many research fields and applications in recent decades. Cold atmospheric plasmas have several components (sometimes also referred to as agents): UV radiation, various species (both charged and neutral, including ions, free radicals, etc.) and electric field. The most important advantage of cold atmospheric plasmas is their ability to create a highly reactive environment without causing thermal damage to the target. Therefore, there are many promising applications of cold atmospheric plasmas in biology, medicine or agriculture. A number of papers studied the plasma ability to inactivate bacteria from surfaces of thermo-sensitive materials [1, 2], food packages [3], various foods [4, 5] or seeds surfaces [6–8]. In medicine, atmospheric plasmas have been tested for various applications in dentistry [9, 10], wound healing [11, 12], tissue proliferation [13] or even cancer treatment [14–20]. In a vast majority of these applications, the interactions of plasma with liquids take place, as water is a part of every living organism. Therefore, the importance of understanding the mechanisms of plasma induced chemistry in water and aqueous solutions is crucial. Despite many positive biomedical effects reported, the exact mechanisms of the interaction of plasma with water and biological targets remain relatively not well understood. The effects of atmospheric plasmas depend on many parameters, such as discharge type, working gas, energy delivered, reactor geometry, plasma-liquid interface, etc. Furthermore, there is a huge variety of biological targets (viruses, bacteria, spores, biofilm, fungi, healthy/cancerous mammalian cells, etc.) that respond to plasma treatments in multiple biochemical/biological ways.

Cold atmospheric plasmas are most typically generated by electrical discharges at atmospheric pressure in noble gases (Ar, He), ambient air or various N_2/O_2 (air-like) gas mixtures. In air-like mixtures, the high electric field of atmospheric plasmas is able to excite, dissociate or ionize air molecules (i.e. N_2 and O_2), thus producing primary reactive species, such as atomic O and N, $^\cdot OH$ radical, excited N_2^* or N_2^+ and O_2^+ ions. By several chemical reactions occurring in the gas phase, various reactive oxygen and nitrogen species (RONS) are generated, e.g. NO, NO_2, N_2O, HNO_2, HNO_3, etc. If the discharge is in the contact with water (or water solution), RONS dissolve in it and induce further chemical reactions resulting into aqueous RONS ($^\cdot OH$, H_2O_2, NO_2^-, NO_3^- or ONOOH) in the plasma treated/activated water (PAW) [21, 22]. The plasma interaction with water is species-specific and transport-limited, which depends on the plasma-liquid interface area. It is important to note that the plasma treated gas and water strongly affect each other. The composition of the gas, where the discharge is generated, affects the production of RONS in the treated water, and vice versa, the presence of water molecules affects the chemical reactions occurring in the gas and also the discharge properties [23–25].

Varying the gas composition enables us to study the chemical effects of the plasma generated species in the gas and water. Vice versa, controlling the chemical effects enables us to optimize parameters for a plasma device for specific applications. Many studies compared the effects of different cold plasma sources [22, 26–29]. Jablonowski et al. [30, 31] varied N_2/O_2 ratio in the shielding gas of Ar radiofrequency plasma jet activating NaCl solution. They observed the strongest pH decrease and the highest NO_2^- and NO_3^- concentrations at 25% O_2 in N_2, and the highest H_2O_2 concentration in pure N_2 or O_2 shielding gas. The same plasma jet with various shielding N_2 or O_2 gases was extensively investigated and applied for multiple biomedical uses, including clinical tests [32, 33]. Similarly, Girard et al. [34] studied the effect of the shielding gas composition of He plasma jet on

RONS composition in phosphate buffer saline solution. They found the highest NO_2^- concentration at 20% O_2 in N_2 shielding gas, and the highest H_2O_2 concentration in pure N_2 shielding gas. Variation of H_2O_2 and NO_2^- concentrations in PAW as a function of N_2/O_2 ratio in He plasma jet were also reported in [35] and [36].

H_2O_2, NO_2^- and NO_3^- are the main, easy to detect, long-lived species in PAW with potential important effects on microorganisms. Numerous studies suggested the importance of the NO_2^- and H_2O_2 synergy [21, 31, 37–39]. Kono et al. [40] reported a mild inactivation of *E. coli* if the NO_2^- or H_2O_2 alone was present in the solution, but their combination enhanced the inactivation of bacteria in dependence on NO_2^- and H_2O_2 concentrations, solution pH and time. Many authors agreed that discharges generated in air or in gas mixtures containing both O_2 and N_2 have higher antibacterial efficiency in comparison to pure O_2 or N_2 gas [31, 41, 42], as they produced both H_2O_2 and NO_2^-. The mutual reaction of H_2O_2 and NO_2^- produces peroxinitrite/peroxynitrous acid ($ONOO^-$/$ONOOH$), that is widely considered to be the species most responsible for the antibacterial effects [21, 31, 37, 41, 43, 44]. The importance of $ONOO^-$/$ONOOH$ lies in its ability to cross the cell membrane and decay inside the cell into cytotoxic reactive species with a subsequent damage of the intracellular structures [31, 41], such as direct oxidation of sulfhydryl groups and initiation of the lipid peroxidation [40]. Therefore, the presence of H_2O_2 and NO_2^- can be an indicator of the antibacterial potential of PAW. Hozák et al. [45] considered the combination of H_2O_2 and NO_3^- to be the active components of PAW produced by positive DC corona discharge in a transient spark regime. Julák et al. and Qi et al. [46, 47] denoted the biological activity of PAW to H_2O_2 in acidic conditions.

While H_2O_2, NO_2^-, NO_3^- and other species and their combinations in PAW have antibacterial effects, direct plasma treatment is generally much more efficient for such effects. This is most likely due to short-lived reactive species. The nature of the species always depends on the exact plasma-liquid-target interaction conditions [48]. Several studies evaluated short-lived reactive species, such as ˙OH radicals and O atoms, that play an important role in bacteria inactivation [49, 50]. Atomic O radicals, generated in the gas plasma can indeed penetrate into the plasma treated liquids [51, 52]. Ikawa et al. [53] and Shaw et al. [54], on other hand, believe that the main factor responsible for the antibacterial activity is peroxynitric acid O_2NOOH through the formation of short-lived $O_2^{\cdot-}$.

In most reported cases of direct plasma treatment, the strongest antibacterial effects were found in air-like mixture or a gas mixture containing both O_2 and N_2. Jablonowski et al. [31] found the most effective inactivation of *E. coli* ~6 log reduction after 10 min by Ar plasma jet at 25% O_2 in N_2 shielding gas and reported no inactivation for pure O_2 or N_2 shielding gas. Ke et al. [41] also observed the highest *E. coli* inactivation ~99% by corona discharge in air-like mixture, compared to pure O_2 or N_2. They observed more severe damage of bacterial cell membrane in air plasma compared to O_2 plasma. Moreover, the direct plasma-induced inactivation was slightly higher than that induced by artificial chemical equivalent solution of acidified NO_2^- and H_2O_2. Chen et al. [55] observed disruption of bacterial membrane, formation of pits, shrinking and distortion on the cell wall after exposing bacteria to air PAW compared to O_2 PAW prepared by micro-hollow cathode discharge. Similarly, Eto et al. [56] observed ~4 log reduction of *G. stearothermophilus* spores at 50% O_2 in N_2 after 5 min direct treatment with dielectric barrier discharge. However, they concluded that UV and O_3 in combination with chemical reactions in water vapor contributed to the sterilizing effect, with a major role of ˙OH radical and O_3. On the contrary, Ke et al. [41] did not find any correlation between bacteria inactivation and ˙OH concentration in (O_2, N_2, air) PAW. They concluded that although the transient species such as ˙OH radical play a role in the direct bacterial inactivation, it is not the main reason

for the difference in antibacterial effects of the plasma generated in various N_2/O_2 gas mixtures. Some studies found effective bacterial inactivation even when plasma was generated in pure N_2. Van Bokhorst-van de Veen et al. [57] showed inactivation of different heat- and chemical-resistant spores by N_2 plasma jet and suggested the important role of reactive nitrogen species in spore inactivation. In dependence on the plasma source and the bacteria strain, other studies came to different conclusions. Abonti et al. [58] investigated the effect of multigas plasma jet (N_2, O_2, Ar, 50% O_2 in N_2) on three types of oral bacteria cultivated on agar plates. The plasma generated in O_2 had the best sterilizing effect on all three types of bacteria due to a higher level of reactive oxygen species (ROS) (O, O_3, $^.$OH, $^1O_2$) that can initiate lipid peroxidation with an increase of membrane fluidity and subsequent cellular leakage. Zhang et al. [50] distinguished the effects of short-lived and long-lived species. They concluded the short-lived reactive species, such as $^.$OH and O atoms, play an important role in bacteria inactivation during the plasma treatment, while long-lived reactive species are responsible for destructive effects on bacteria during a longer time that is needed for better indirect inactivation effects after treatment.

The plasma effect on bacteria depends on various parameters, such as plasma source (plasma jet, DBD, micro hollow, corona, spark discharge), discharge reactor geometry and contact with water, gas mixture and water solution composition. Moreover, the plasma induced effect also depends on the microorganism type, its metabolism and protection against stress conditions. Therefore, it is crucial to know the concentrations of species produced by the plasma in the gas phase, understand their subsequent transport into water and know the concentrations of reactive species in water. It is likely that antibacterial effects are not the result of single reactive species action, but rather a combination of various species determined mainly by discharge properties and gas mixture composition.

The objective of this study was to investigate the effect of gas composition (N_2/O_2 ratio in nitrogen/oxygen mixtures) on the production of RONS in gas and in water and subsequent effects on bacteria, to deeper understand the interaction of cold air plasma with bacteria. Particularly, we investigate the effect of transient spark discharge that has been extensively studied in air but not in various N_2/O_2 gas mixtures. The advantage of transient spark discharge is that it works in non-expensive diatomic gases N_2/O_2 at atmospheric pressure, compared to widely used but relatively expensive noble gas plasma jets. We study the production of reactive species in the gas and subsequently in PAW in dependence on the N_2/O_2 ratio, the gas flow rate and water treatment time. The effect of the humidity on the production of gaseous RONS is also studied by comparing the results with and without water circulating in the system. Besides analyzing RONS such as H_2O_2, NO_2^- or NO_3^- in water in dependence on the gas mixture composition, we also monitor $^.$OH radical production, for the first time with transient spark discharge in various N_2/O_2 mixtures. The overall effect on Gram-negative bacteria *E. coli* is investigated in pure O_2 gas, air-like mixture (20% of O_2 in N_2) and in pure N_2 gas in order to better clarify the cold plasma components responsible for bacterial inactivation. The correlation between gaseous species, reactive species in the PAW and bacterial inactivation in the individual gas mixtures is discussed.

Experimental Setup

The experimental setup is schematically depicted in Fig. 1. It consists of a plasma reactor, equipped with high voltage–power supply and necessary electrical diagnostics, gas and water containers and driving systems, systems for gas and water analysis, as well as, the analysis of antibacterial effects.

Plasma Reactor, Electrical Circuit and Diagnostics

The plasma reactor (Fig. 1) of a point-to-plane geometry consisted of a hypodermic needle used as a high voltage electrode placed above the grounded electrode. The grounded electrode was embedded in a narrow channel (width and length was 1 and 31 mm, respectively) in the inclined PTFE element (dimensions 31×28 mm, angle of inclination 45°) to allow driving water down the electrode. The electrodes were made of stainless steel and their distance was kept constant at 1 cm. The system was enclosed in a small acrylic chamber (volume ~ 1 mL) equipped with gas and water inlets and outlets.

The plasma was generated by a transient spark (TS) discharge. The TS is a DC-driven self-pulsing repetitive streamer to spark transition discharge. It has been studied and described in detail in our previous works [59–62]. The discharge was driven by positive DC high voltage–power supply (*Technix S20-R-1200*) and its electrical characteristic were monitored by high voltage probe (*Tektronix P6015A*) and Rogowski type current probe (*Pearson Electronics 2877*) connected to a digitizing oscilloscope (*Tektronix TDS 2024*).
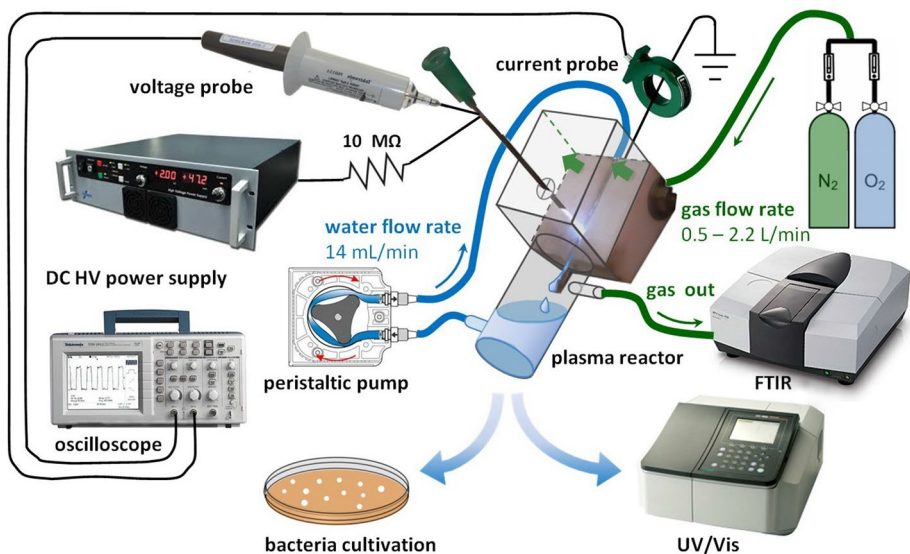

Fig. 1 Schematic of the experimental setup

Gas Mixtures and Water

The gas cylinders of nitrogen N_2 (purity 4.0) and oxygen O_2 (purity 2.5) were used to prepare various gas mixtures: 0, 10, 20, 50, 80, and 100% of O_2 in N_2. The gas mixture was driven via PTFE tubes to the reactor and then from the reactor to the FTIR spectrometer for the gas analysis. The gas flow rate was controlled by the gas rotameters (*Aalborg*) in the range of 0.25–2.2 L/min.

We used a non-buffered 7.5 mM monosodium phosphate $NaH_2PO_4 \cdot 2H_2O$ solution (conductivity 600 μS cm^{-1}, pH 5) that mimics the conductivity of tap water (further referred only as *water,* this solution was used also in our previous papers, e.g. [22, 37]). The solution was prepared by dissolving adequate amounts of $NaH_2PO_4 \cdot 2H_2O$ in the respective volume of deionized water prepared by reverse osmotic system (*Aqua Osmotic Type 02*). The water was in a container attached to the acrylic chamber placed at the bottom of the PTFE element. A peristaltic pump (*Masterflex L/S*) was used to pump the water from the container to a top of a channel in the element with a constant flow rate of 14 mL/min. The water was flown down the element where it was treated by a discharge and then dropped down and was collected in the container.

We used constant volume of water sample (5 mL) and treated it by plasma at two specific times (5 or 10 min) by TS discharge.

Gas Analysis

The chemical analysis of gaseous species produced by the TS discharge was done by FTIR absorption spectroscopy (*Shimadzu IRAffinity-1S*) using a 10 cm long gas cell with CaF$_2$ windows. The spectra measurement was performed in the middle infrared region of 4000–1000 cm^{-1} with a 0.5 cm^{-1} spectral resolution. The analyzing chamber of the spectrometer was purged by high purity (5.2) nitrogen to minimize the effect of the ambient humidity on the measured spectra. The FTIR spectra allowed for identification of various species generated by TS discharge in the gas phase, both qualitatively and quantitatively. The concentrations of main gaseous species, such as nitric oxide NO, nitrogen dioxide NO_2, nitrous oxide N_2O and ozone O_3 were evaluated in absolute (ppm) units based on previous FTIR calibrations. The concentration of nitrous acid HNO_2 was evaluated based on spectrum generated using absorption cross sections for HNO_2 obtained from HITRAN database [hitran.org] and deconvoluted to the same spectral resolution to fit it to our measured spectra.

Water Analysis

The interaction of the TS discharge with water solutions leads to an efficient mass transfer of plasma-generated gaseous reactive species through the plasma-liquid interface into water and subsequent formation of various aqueous RONS in PAW. Among the main aqueous species hydrogen peroxide H_2O_2, nitrite NO_2^- and nitrate NO_3^- were detected and their absolute concentrations were evaluated by colorimetric methods based on UV–Vis absorption spectroscopy (*Shimadzu UV-1800*). For the analysis of hydroxyl radical $^{\cdot}OH$ we used fluorescence spectroscopy (*Shimadzu RF-6000*).

Concentration of H_2O_2 was evaluated by titanium oxysulfate TiOSO$_4$ assay under acidic conditions (4 g/L TiOSO$_4$ 1:1 with concentrated H_2SO_4) [21, 37, 63]. The reaction of titanyl ions Ti^{4+} with H_2O_2 leads to formation of yellow-colored complex of pertitanic acid

H_2TiO_4 with the absorption maximum at 407 nm. The color intensity is proportional to the H_2O_2 concentration. To prevent the H_2O_2 decomposition by the reaction with NO_2^- under acidic conditions, after the discharge treatment the sample was immediately stabilized by 60 mM sodium azide NaN_3. Sodium azide reduces NO_2^- into molecular N_2 and preserves the H_2O_2 concentration intact [37]. The used volume ratio of sample:NaN_3:$TiOSO_4$ was 10:1:5.

Concentrations of NO_2^- and NO_3^- were evaluated by Griess reagents under acidic conditions [64, 65] using the chemicals and according to protocol (*Cayman Chemicals Nitrate/ Nitrite Colorimetric Assay Kit # 780001*). This method is easy to perform and approved as precise for NO_x^- measurement in the PAW produced by TS discharge [66]. The reaction of nitrites (NO_2^-) with the Griess reagents leads to formation of deep purple azo compound with the absorption maximum at 540 nm. Nitrates (NO_3^-) were converted into NO_2^- by using the nitrate reductase enzyme with cofactor and subsequently analyzed the same way as NO_2^-. By this procedure the total concentration of NO_2^- plus NO_3^- is evaluated, after subtracting NO_2^- concentration it gives the NO_3^- concentration. If the concentration of NO_x^- was too high, we diluted the sample with deionized water to adjust the NO_x^- concentration in the linear absorbance range.

For the $\cdot OH$ radical measurement we tested two fluorescent probes - terephthalic acid (TA) and coumarin that have highly specific reaction towards $\cdot OH$ radical [67]. Both molecules are non-fluorescent, only after a contact with $\cdot OH$ radical they can be easily hydroxylated, and their products (hydroxyterephthalic acid (HTA) or hydroxycoumarin) are fluorescent. Both $\cdot OH$ radical probes have certain advantages and disadvantages. Coumarin is highly soluble in water, however, the produced hydroxycoumarin can be easily decomposed by the TS discharge and therefore, it is not suitable for $\cdot OH$ radical evaluation in our experiment. On the contrary, hydroxyterephthalic acid (HTA) is more stable and because of the TA molecule symmetry only one isomer is formed by its hydroxylation [68]. Therefore we used TA as a probe for $\cdot OH$ radical evaluation. As TA is soluble only in basic solutions, 2 mM TA was dissolved in 5 mM NaOH solution (initial pH 10). Due to a very short lifetime of $\cdot OH$ radicals, TA was added into the NaOH solution prior to the treatment. The concentration of HTA in solution after plasma treatment was analyzed by the fluorescence spectrometry with excitation and emission wavelengths 310 nm and 425 nm, respectively [69]. As HTA can also be produced from TA by photochemical reactions, the solution of TA was always stored in dark conditions. The blank fluorescence of TA was equivalent to 40 nM of HTA. The $\cdot OH$ radical concentration could be evaluated according to the calibration of HTA solution with fluorescence proportional to the $\cdot OH$ radical concentration. Mark et al. [70] estimated the efficiency of TA reaction with $\cdot OH$ radical to 35%.

However, in our PAW conditions where many RONS are present and may interact with $\cdot OH$ radical and TA, we cannot reliably measure the $\cdot OH$ radical absolute concentration, since selectivity/specificity of TA reaction with $\cdot OH$ may be significantly affected. Moreover, $\cdot OH$ radicals and O atoms often have comparable reactivity, and in case of hydroxylation of aromatics they may result in the same compounds. Therefore, HTA can be a product of $TA + \cdot OH$, as well as of $TA + O$ atoms. O atoms are widely generated in the O_2-containing plasmas and can be transported into plasma treated liquids [52]. This means that a substantial part of the measured HTA can be due to the presence of O atoms, and not only $\cdot OH$ radicals. As a consequence, using TA as a probe we can only measure the relative $\cdot OH$ radical concentration.

In summary, we measured absolute concentrations of H_2O_2, NO_2^- and NO_3^- in water solution, and relative $\cdot OH$ radical concentration (represented as HTA fluorescence) in $TA + NaOH$ solution. To be able to relate the production of these species in water with the

$^{.}$OH production, we also measured concentrations of H_2O_2, NO_2^- and NO_3^- in the plasma treated NaOH with and without TA, and subsequently also monitored pH changes as a function of the gas mixture.

Antibacterial Effects

Antibacterial effects of the TS discharge were investigated on Gram-negative bacteria *Escherichia coli* (ATCC 25922/CCM 3954). Planktonic bacterial water suspension, i.e. bacteria floating in the solution was used for experiments. The initial concentration of bacteria in solutions was $\sim 10^7$ colony forming units per mL (CFU/mL). The bacterial solution after plasma treatment was serially diluted and finally 100 μL of the solution was spread on agar plates. The plates were cultivated at reverse position at 37 °C overnight. As viable we consider those bacteria which reproduced to form a colony visible by naked eye. The bacterial inactivation was evaluated by standard colony counting method and inactivation effect was expressed as a logarithmic reduction of bacterial concentration. A test of vulnerability of *E. coli* to elevated temperatures and a water flow has been done (5 mL of solution was circulated for 10 min at 40 and 60 °C) but showed no antibacterial effect.

Data obtained from the measurements are presented as mean values ± standard deviations.

Experimental Results and Discussion

The results and discussion are divided into five sections dealing with the properties of TS generated in various N_2/O_2 gas mixtures; chemical species formed by TS in the gas without water flow; chemical species formed by TS in the gas with water flow; chemical species formed in the water and finally antibacterial effects induced by the plasma treated water.

Discharge Properties

In all experiments a transient spark (TS) discharge of positive polarity was used. TS is typical with current pulses of high amplitude (order of several A) and very short duration (10–100 ns), and frequency of the order of several kHz. During the current pulses the breakdown voltage drops almost to zero, as the electric circuit internal capacity discharges completely. After the breakdown, the potential across the discharge gap starts to increase as the capacity recharges until another breakdown occurs.

In our experiments, the typical amplitude of the applied voltage from the power supply was $U_{app} = 16$–17 kV, amplitude of the breakdown voltage was $U_{br} = 7$–12 kV, average discharge power was $P \sim 4.5$–7 W, and amplitude and frequency of the discharge current pulses were $I_{max} = 2$–7 A and $f = 2$–3 kHz, respectively. These values varied with the gas mixture composition, i.e. N_2/O_2 ratio and are presented in Table 1. They were also slightly different in systems with and without the water flow. The amplitude of the current pulses typically increased with the increase of O_2 in N_2. In pure O_2 the amplitude was the highest (~ 5 to 7 A), while in pure N_2 it was the lowest (~ 2.4 to 3 A). On the contrary, the frequency of the discharge pulses was higher (~ 2 to 4 kHz) and less regular in pure N_2, while in pure O_2 it dropped to ~ 1.7 to 2 kHz and was quite regular. As a result, the average discharge power in various gas mixtures was not equal. The highest average power ~ 7 W was in the mixtures containing both O_2 and N_2. As the discharge power may influence the chemical effects in

Table 1 Summary of the typical discharge characteristics in various N_2/O_2 mixtures with water circulating in the system

	0% O_2 (100% N_2)	20% O_2	50% O_2	100% O_2
U_{br} [kV]	7–10	8–10	8–10	11–12
I_{max} [A]	2.4–3	3.3–4.3	3–4	5–7
f [kHz]	2–4	2.6–2.8	2–3	1.7–2
P [W]	~4.5	~6.9	~7	~5.8

both gas and water, its stabilization is very important. In the case of TS discharge, that is a self-pulsing repetitive streamer to spark transition discharge, it represents a real challenge. Especially when one must keep in mind that the gas mixture strongly influences not only the frequency of the discharge pulses, but also the overall discharge stability.

The water solution was initially of room temperature, however, extended treatment by the TS discharge lead to an increase of temperature and evaporation of the water. For example, with 10 min treatment time the temperature of water increased by 4.1 ± 1.5 °C and approximately ~10% of its volume was evaporated.

Chemical Species in Gas Mixtures without Water Flow

When plasma is generated in air at atmospheric pressure it produces high energy electrons that can effectively excite, dissociate or ionize air molecules. The emission of O, N and N^+ atomic lines, $N_2(C)$ second positive system and also $N_2^+(B)$ first negative system at higher discharge pulse frequencies were identified as dominant species in TS discharge generated in atmospheric pressure air [59, 61]. Beside these radiative species, other species were also produced. Here we discuss only those that are relevant for the chemical processes in the gaseous N_2/O_2 mixtures and water.

The cold air discharge plasma reactivity is initiated with electrons that break the double bonded O_2 more easily than the triple bonded N_2, therefore the atomic oxygen O and excited nitrogen molecules N_2^* are mostly formed as primary species. Excited N_2^* can be easily dissociatively quenched by molecular O_2 thus producing additional atomic O. High energy electrons can also ionize N_2 and O_2 molecules and produce O_2^+ and N_2^+ ions. Those may further react via dissociative electron–ion recombination and form atomic O and N. Atomic O and N are essential for a production of nitric oxide NO that most probably occurs via Zeldovich mechanism ($O + N_2 \rightarrow NO + N$ and $N + O_2 \rightarrow NO + O$) [71]. Although the TS discharge generates cold plasma, the temperature can be high enough during the spark phase to consider Zeldovich thermal mechanism of NO_x production [62]. The atomic O also contributes to the NO oxidation into nitrogen dioxide NO_2. NO can be also oxidized by O_2 and especially O_3 that contributes to the increase of the overall NO_2 concentration in the gas. In air-like mixtures treated by the TS discharge, NO and NO_2 are dominant gaseous species that is also shown by FTIR spectrum (Fig. 2). Figure 3 shows concentrations of NO and NO_2 as a function of gas composition (N_2/O_2 ratio) without water flow. The NO and NO_2 concentrations increased with O_2 up to 50%, where they reached a maximum 764 ppm and 302 ppm, respectively, at gas flow rate 0.5 L/min. With further increase of O_2 in the mixture, the concentration of NO and NO_2 decreased. In all gas mixtures the absolute concentration of NO was higher than the concentration of NO_2. The reason is that the primary product of Zeldovich mechanism is NO, while NO_2 is formed by later oxidation of NO.
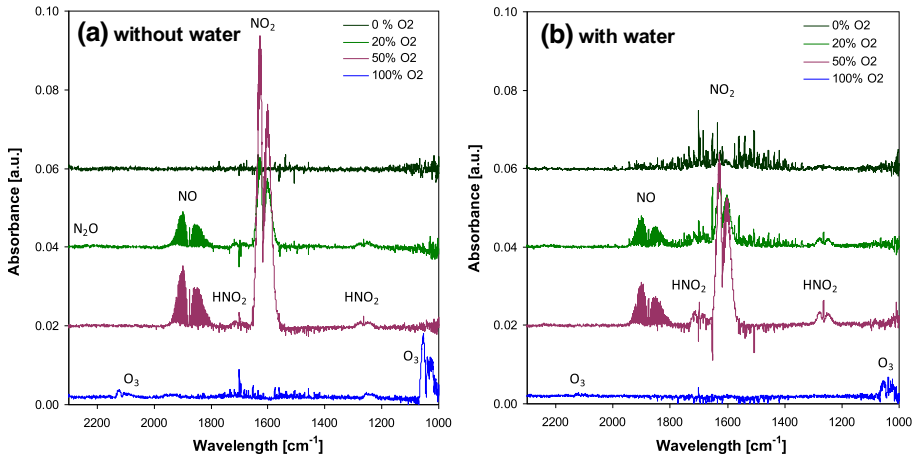
Fig. 2 FTIR absorption spectra of gaseous products generated by TS discharge in various gas mixtures (N_2/O_2 ratio) [gas flow rate Q = 0.5 L/min] without water (**a**) and with water (**b**) in the reactor
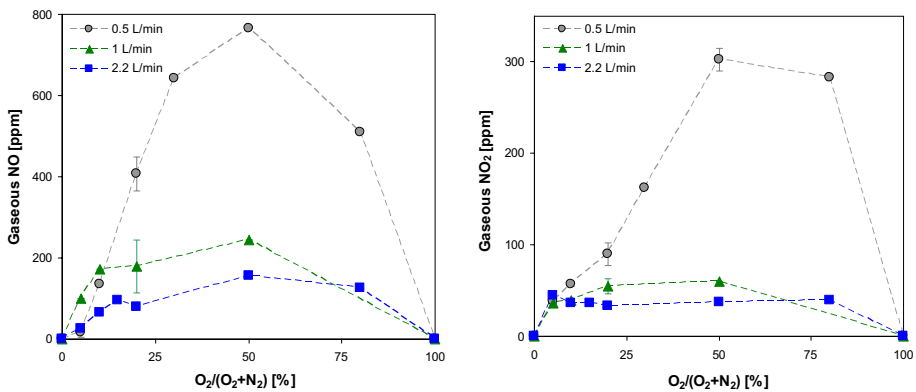

Fig. 3 Concentrations of NO and NO_2 in gas phase as a function of gas mixture (N_2/O_2 ratio) and gas flow rate Q without water flow

Figure 3 also shows that with an increasing gas flow rate, the concentrations of NO and NO_2 in the gas decreased. It is a result of shorter residence time of gas mixture in the discharge zone, i.e. decrease of the energy deposited per volume of the gas. The NO/NO_2 concentration can be also influenced by other discharge parameters, especially those affecting the deposited energy. In the previous works from our group [22, 62] we monitored concentration of NO and NO_2 in the gas phase as a function of increasing frequency of the TS current pulses (data not shown) and found that NO increased faster than NO_2 with increasing pulse frequency, i.e. with the total energy delivered into the plasma by TS pulses.

In addition to NO and NO_2, trace amounts of nitrous oxide N_2O were observed in the FTIR spectra without water flow (Fig. 2 a). N_2O concentration was also evaluated with respect to the gas mixture composition (Fig. 4). The highest concentration (3.5 ppm) was observed for the lowest O_2 concentration (5%) in N_2. In gas mixtures containing mainly N_2

Fig. 4 Concentration of N_2O produced by TS discharge in the gas phase as a function of gas mixture (N_2/O_2 ratio) [dry gas, $Q = 0.5$ L/min, $f = 2.5$ kHz]
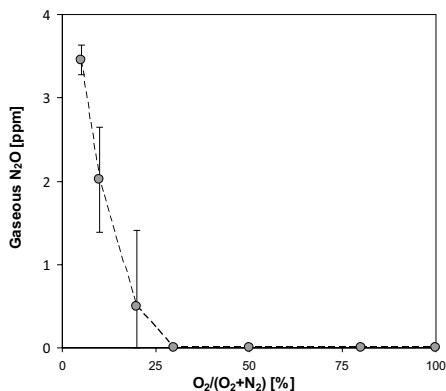
(when O_2 concentration is below 20% O_2), the most possible production of N_2O occurs via reaction of $N^.$ with NO_2 ($N^. + NO_2 \rightarrow N_2O + O^.$) or eventually via reaction of N_2^* with O_2 ($N_2(A^3\Sigma_u^+) + O_2 \rightarrow N_2O + O$) [72–74]. In gas mixtures containing higher O_2 concentration, N_2O depletes during thermal decomposition into N_2 and O_2 or NO, thus contributing to NO concentration prevalence ($N_2O + O \rightarrow N_2 + O_2$; $N_2O + O \rightarrow 2NO$) [75]. With respect to low concentrations of N_2O compared to NO and NO_2, it can be assumed that its contribution to the overall chemistry in gas and water, as well as its antibacterial effects, are probably negligible.

The production of atomic oxygen $O(^3P)$ can also lead to the formation of ozone O_3 via 3-body reaction ($O + O_2 + M \rightarrow O_3 + M$). This mechanism is efficient especially at lower gas temperatures, i.e. further away from the plasma channel. In TS discharge generated in air, however, the concentration of O_3 is negligible, as during the spark phase the increase of gas temperature causes a rapid decomposition of O_3. Moreover, in the presence of NO that is efficiently produced in TS, O_3 would readily oxidize NO resulting into NO_2 [22]. Ozone in the gas phase was detected only if TS discharge was generated in pure O_2 both with and without water flow (Fig. 2). Its concentration in dry O_2 at gas flow 0.5 L/min reached 207 ppm. In pure O_2, neither NO, NO_2 nor other gaseous species were found in FTIR spectra, only O_3. NO and NO_2 were also not detected in FTIR spectrum when pure N_2 was used. In general, in pure N_2 there were no species that could be detectable by FTIR spectroscopy in our experiments.

Chemical Species in Gas Mixtures with Water Flow

If water molecules are present in the discharge zone, the reaction mechanism presented in the previous section must also consider the effect of highly reactive species such as $^.OH$, $H^.$ and $HO_2^.$ radicals. In our experimental system water is circulated by a peristaltic pump down the inclined grounded electrode and treated by TS discharge.

The hydroxyl radicals $^.OH$ can be generated via several possible reactions, mainly by dissociation of H_2O induced by electrons or by atomic oxygen $O(^1D)$ or excited metastable molecules $N_2^*(A)$. In addition, $^.OH$ radicals can also be produced by a subsequent reaction of $H^.$ radical with atomic O. On the contrary, $^.OH$ concentration may decay via 3-body recombination producing hydrogen peroxide H_2O_2. The production of $^.OH$ radicals in atmospheric air treated by TS discharge was confirmed by optical emission spectroscopy [59].

In the presence of water that leads to $^{\cdot}$OH radical production, other pathways for NO formation are possible when compared to dry gas N_2/O_2 mixture. Besides NO formation via above-mentioned Zeldovich mechanism, it can be also formed via reactions of atomic N with $^{\cdot}$OH radical [76]. When H_2O molecules are present in the gas phase, NO can be oxidized by $HO_2^{\cdot}$ further to NO_2 and contribute to NO depletion, yielding $^{\cdot}$OH radicals ($NO + HO_2^{\cdot} \rightarrow {}^{\cdot}OH + NO_2$) [77–79]. The $HO_2^{\cdot}$ radicals can be produced via mutual reactions of OH, O_3 and H_2O_2 (e.g. $OH + H_2O_2 \rightarrow HO_2^{\cdot} + H_2O$ [14, 78, 80, 81], $O_3 + H_2O_2 \rightarrow {}^{\cdot}OH + HO_2^{\cdot} + O_2$ [79] or $O_3 + {}^{\cdot}OH \rightarrow HO_2^{\cdot} + O_2$ [82]), although reactions including H_2O, O or O_2 leading to $HO_2^{\cdot}$ formation are also possible [83]. Further, $^{\cdot}$OH radicals are essential for further 3-body oxidation of NO and NO_2 to nitrous acid HNO_2 and nitric acid HNO_3, respectively [79, 84].

Figure 5 shows concentrations of NO and NO_2 in the gas phase of the discharge in a contact with water as a function of N_2/O_2 ratio. We observed a similar dependence (profile) of NO and NO_2 concentrations on N_2/O_2 ratio as in the system without water (Fig. 3), although the absolute concentrations with water are lower (Fig. 5). For example, NO concentration at 50% O_2 in N_2 with and without water was 570 and 764 ppm, respectively. In the same case, NO_2 concentration with and without water was 165 and 302 ppm, respectively. The main reason for lower concentrations with water flow is that NO and NO_2 are oxidized by $^{\cdot}$OH to HNO_2 or HNO_3. Some of NO and NO_2 also directly dissolve into water. We found higher concentration of HNO_2 in the gas mixtures with water (3.4 ppm) compared to dry gas mixtures (1.7 ppm) at 50% O_2 in N_2 at 0.5 L/min gas flow. The concentration of HNO_2 had a similar profile as NO, NO_2 concentrations displayed as a function of N_2/O_2 ratio, i.e. it increased up to 50% O_2 in N_2 and then decreased (Fig. 5). With the increasing gas flow rate, the concentrations of all gaseous species (NO, NO_2, HNO_2) in the mixtures with water decreased (data not shown). Similar effect of the gas flow rate was also observed in dry gas mixtures and is shown in Fig. 3. Besides NO, NO_2 and HNO_2 no other nitrogen species were detected in the FTIR spectra. Traces of N_2O or HNO_3 were expected, but they were not recognized in the spectra, or their concentration was below the detection limit.

Formation of O_3 in gas phase was observed only in pure O_2. The O_3 concentration in O_2 with water was smaller (125 ppm) when compared to dry O_2 (207 ppm). In O_2 atmosphere with water, some of the formed O_3 dissolves into the water despite its relatively low Henry's law solubility constants [22, 85]. In addition, the presence of water and especially N_2 in the gas suppressed the concentration of the generated O_3. It is in agreement with the

Fig. 5 Concentrations of NO, NO_2 and HNO_2 in gas phase as a function of gas mixture (N_2/O_2 ratio) with water flow [gas flow rate Q = 0.5 L/min]
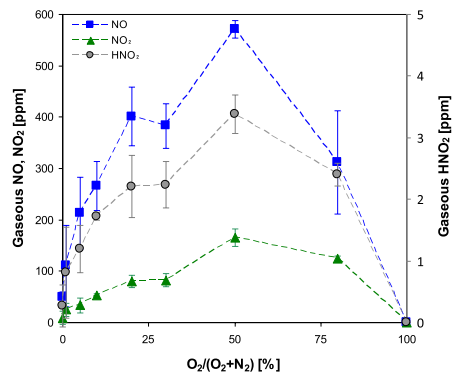
fact that maximal O_3 concentration can be achieved in pure O_2, and it decreases with any impurity or admixture present in the system [86]. In gas mixtures where N_2 is present, O_3 decay is associated with NO oxidation to NO_2, as explained above. In the gas mixtures with water vapours, O_3 decay can also happen via a rapid reaction with $^.$OH radicals ($O_3 + ^.OH \rightarrow HO_2^. + O_2$) [82]. These O_3 decay mechanisms are probably the reason why we did not detect any O_3 in PAW, not even in pure O_2 with water. Even if some O_3 was formed and dissolved in water, its concentration was probably very small and below the detection limit of the used indigo trisulphonate method (0.1 μM [87]). More details on O_3 in water solution are discussed in section "Chemical Species in Water" and in [66]. The gas species chemistry in humid air mixtures has been described in more detail in [22].

If the discharge was generated in pure N_2 with water, we detected small concentrations of NO, NO_2 and HNO_2 in the gas phase: 49.3 ppm NO and 9.2 ppm NO_2 (Fig. 5). On the contrary, in pure N_2 without water none of them was detected. The source of O and $^.$OH necessary for NO_x formation in pure N_2 is probably from the H_2O dissociation by TS discharge. Therefore, NO_x and HNO_x can be found in pure N_2 with water, but not without water. Another source of atomic O necessary for NO_x formation can be molecular O_2 dissolved in water. Similar to gas mixtures with various N_2/O_2 ratio, also in pure N_2 the measured concentrations of NO and NO_2 in the gas are affected by their partial dissolution in the PAW.

One could expect formation of some ammonia NH_3 in N_2 discharge with water vapours [88], and perhaps even in minor amounts in N_2/O_2 mixtures [89]. Indeed, some weak NH bands have been detected in the emission spectrum of a similar TS discharge in ambient air [62]. However, no NH_3 has been detected in FTIR spectra in either of the gas mixtures studied, which might be due to its probably very low concentration (detection limit 20 ppm), as well as overlapping with H_2O absorption bands.

In pure O_2 the situation is completely different as here none of NO, NO_2 and HNO_2 were detected both with and without water. While in pure N_2 the water is a source of oxygen, in pure O_2 there is no natural source of N necessary for NO_x formation. In addition, solubility of molecular N_2 ($k_H = 6.5 \times 10^{-4}$ M/atm) is two times smaller than of O_2 ($k_H = 1.3 \times 10^{-3}$ M/atm) [85] so N_2 cannot serve as a sufficient N source for NO_x formation in pure O_2 either.

Apart from NO, NO_2 and HNO_2 we did not detect any N_2O in any gas mixture when discharge was operated in contact with water. The reason can be that $^.$OH and H$^.$ radicals may rapidly decompose N_2O ($N_2O + H^. \rightarrow N_2 + ^.OH$, $N_2O + ^.OH \rightarrow N_2 + HO_2^.$) [79, 90].

Lower measured concentrations of various gaseous species produced in the gas phase with water compared to the conditions without water are due to the solvation of gaseous species in water, depending on their Henry's law solubility constants. These solvation mechanisms are coupled with the chemical reactions. We admit that the complexity is large, and our current knowledge on exact gas phase and liquid phase chemistry with respect to transport of plasma generated species into water is limited. Therefore, along with the analysis of the gaseous products we also measured and evaluated the concentration of selected reactive species (H_2O_2, NO_2^-, NO_3^- and $^.$OH) in PAW, and we monitored the pH of PAW. These results are presented in section "Chemical Species in Water".

Chemical Species in Water

Details on the air plasma induced chemistry in water were published in [22, 23, 25, 37, 66, 91, 92]. Many of chemical species in the water phase originate in the gas phase [91, 92].

Hydrogen peroxide H_2O_2 is produced mostly in the gas phase by a 3-body recombination of ·OH radicals and subsequently dissolved into water very quickly due to its high Henry's law solubility ($k_H = 7.1 \times 10^4$ M/atm). However, H_2O_2 can also be formed directly in water, again by recombination of ·OH radicals in a 2-body reaction.

Gaseous NO and NO_2 dissolve and react with water producing nitrites NO_2^- and nitrates NO_3^- and H^+ [93]. Involvement of other oxidizing species (e.g. $O_2/O/O_3/OOH$) in the production of NO_2^- and NO_3^- is probable too. HNO_2 and HNO_3 produced in gas phase (HNO_3 is formed dominantly by ·$OH + NO_2 \rightarrow HNO_3$ [73]) also easily dissolve into H_2O and contribute to NO_2^- and NO_3^- formation in water and further decrease of pH (formation of H_3O^+). Formations of NO_2^- and NO_3^- in water solution are considered as main reactions responsible for PAW acidification, i.e. decrease of pH associated with the release of H^+ (H_3O^+). The acidity of the PAW and its buffering capacity is crucial for further chemical reactions. The NO_2^- at low pH (below $pK_a = 3.4$) is dominantly in the form of non-dissociated nitrous acid HNO_2 [94] that is unstable and disproportionates directly, or through series of reactions (including intermediate products NO· and $NO_2^·$) into NO_3^- [93], which contributes to eventually higher concentrations of NO_3^- than NO_2^- in acidic PAW. At higher pH (above 3.4) nitrite takes form of a dissociated anion NO_2^-. The intermediates NO· and $NO_2^·$ are known for their strong cytotoxic effects [38, 43]. Moreover, even in mildly acidic conditions, NO_2^- reacts with H_2O_2 to produce peroxynitrites (or peroxynitrous acid) $O=NOO^-$ ($O=NOOH$, $pK_a = 6.8$) that is also known for its strong cytotoxic effects [14, 21, 37, 95]. Other pathways leading to formation of peroxynitrites are via reactions among radicals ·OH, $NO_2^·$, $O_2^{·-}$, NO·. At acidic pH peroxynitrites are very unstable and quickly decompose to ·OH and $NO_2^·$, as well as into NO_3^-. At pH close to neutral they could decay through the series of reactions into NO_2^- [91, 96, 97]. All RONS are important as they may cause cell membrane peroxidation, especially at low pH, and play an important role in antibacterial activity of PAW.

Figure 6 shows concentrations of H_2O_2, NO_2^- and NO_3^- in PAW as a function of gas mixture with water treatment time 10 min. In pure N_2 they were 0.9 mM, 0.4 mM and 0.7 mM, respectively. These concentrations changed with the increase of the O_2 in gas mixture. The concentration of H_2O_2 and pH decreased and reached minimum at 50% O_2 in N_2, 0.4 mM and 2.9, respectively. On the other hand, concentrations of NO_2^- and NO_3^- increased and reached 0.7 and 4.0 mM, respectively, at approximately the same N_2/O_2 ratio. Then, with the further increase of O_2 in N_2 (from 50% up to 100%) the trends change, with H_2O_2 and pH increasing again and NO_2^- and NO_3^- decreasing. In pure O_2, no NO_2^- and NO_3^- were detected, while H_2O_2 reached maximum of 1.8 mM and we also observed

Fig. 6 Concentrations of H_2O_2, NO_2^- and NO_3^- and pH in PAW as a function of gas mixture (N_2/O_2 ratio) [gas flow rate $Q = 0.5$ L/min, water treatment time 10 min]
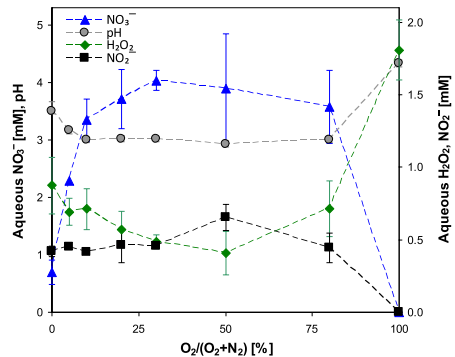
the weakest decrease of pH (from 5 to 4.3 only). In general, the trend of NO_3^- as a function of N_2/O_2 is very similar to the one of NO_2^-, although absolute concentrations of NO_3^- are much higher as usual in non-buffered solutions where significant pH decrease occurs that favours disproportionation of NO_2^- into NO_3^-. The trend of H_2O_2 is completely opposite to NO_2^- and NO_3^-, as conditions that favour NO_x^- formation are not optimal for H_2O_2 production. H_2O_2 is more effectively produced in pure gases (especially pure O_2), when NO_x^- production is minimal. This is dominantly because NO_2^- do not deplete H_2O_2 by their mutual reaction leading to peroxynitrites.

In pure N_2 with water, only small concentrations of NO, NO_2 or HNO_2 were detected in the gas phase by FTIR measurements (Fig. 5). However, in N_2 plasma treated water we measured considerable RONS concentrations (H_2O_2, NO_2^-, NO_3^- and $^{.}OH$) and a decrease of pH (Fig. 6). In the previous section "Chemical Species in Gas Mixtures with Water Flow" we explained that the O/O_2 necessary for formation of NO_x in the gas and NO_x^- in water may come from H_2O dissociation and also from O_2 dissolved in water or impurities in the gas mixture. Dissociation of H_2O molecules may in general occur by high-energy electrons, metastable molecules $N_2(A)$ or photo-dissociation by UV radiation that yields to $^{.}OH$ radical formation in PAW [1, 31]. The metastable molecules $N_2(A)$ were considered dominant species responsible for $^{.}OH$ radical formation in PB solutions treated by He plasma jet with N_2 shielding gas [34, 84] and this may similarly occur in our system in pure N_2 with H_2O. On the other hand, UV radiation emitted by TS plasma is relatively weak [37], so H_2O photodissociation is probably not important in our experimental conditions.

Since NH_3 can be hypothetically produced in N_2 plasma with H_2O (and in minor amounts possibly also in N_2/O_2 mixtures with H_2O [89]), and its dissolution into water is relatively significant ($k_H = 5.9 \times 10^{-1}$ mol m^{-3} Pa^{-1} [85]), we attempted to measure its concentration in PAW by using the testing strips based on Nessler's reagent. However, the sensitivity of testing strips is too low and allowed us to measure NH_3 concentrations as low as 0.5 mM only. No NH_3 has been detected by this method, which means that even if present, its concentration was below the detection limit.

When the discharge was generated in pure O_2 we detected only $^{.}OH$ radical and H_2O_2 but no O_3, NO_2^- or NO_3^- in water solutions. The concentration of the formed H_2O_2 was relatively high (1.8 mM) as a result of a higher formation of $^{.}OH$ radicals (Fig. 6). H_2O_2 accumulated in PAW due to the lack of NO_2^- it could potentially react with. In pure O_2, ozone is a dominant gaseous product and it could partially dissolve into water. However, a brief test with indigo trisulphonate did not indicate any O_3 in the PAW (detection limit 0.1 μM). O_3 is unstable mainly in neutral and basic solutions, when it may react with H_2O_2 and decompose into $^{.}OH$ radical ($O_3 + H_2O_2 \rightarrow {}^{.}OH + HO_2^{.} + O_2$) via Peroxone process [93]. The process results into a decay of both H_2O_2 and O_3 in water [21]. In our case, this process might only contribute when PAW was generated in pure O_2 where the highest concentrations of O_3 in gas, H_2O_2 in water and the highest pH were observed, if compared to other N_2/O_2 gas mixtures. However, as the Peroxone process is effective at pH > 5 and not much O_3 was detected in the gas phase that would dissolve in water, it probably does not play an important role in the TS discharge induced water chemistry.

Besides the effect of N_2/O_2 ratio, we also investigated the effect of gas and water flow rates on gaseous and aqueous chemistry. In the gas mixtures without water we have shown the effect of the gas flow rate on the gaseous chemistry was significant (Fig. 3). In the water (data not shown), NO_2^- concentration decreased, while H_2O_2 concentration and pH increased with the gas flow rate increasing from 0.25 to 2 L/min. The biggest change was observed between 0.25 and 0.5 L/min. With its further increase from 0.5 to 2 L/min, the changes in produced species concentrations were much smaller. The decrease of NO_2^-

concentration corresponds to a decrease of NO_x concentrations in the gas with increasing gas flow rate as a result of shorter residence time, as shown in Fig. 3. Moreover, NO_2^- depletion in the reaction with H_2O_2 (leading to ONOOH formation) can also play a role. As it was also observed in buffered solutions at pH ~ 7 [37, 66], at lower NO_2^- concentration, the H_2O_2 concentration was always higher, since it was not so effectively depleted by the reaction with NO_2^-. Perhaps fewer NO_x produced in the gas phase (with faster gas flow rate) saved more ·OH from dissociated water molecules, which then formed more aqueous H_2O_2. With more NO_x in the gas (with slower gas flow rate), the formation of HNO_x was supported on the expense of ·OH, which resulted in less H_2O_2 in water.

While the effect of the gas flow rate was found significant with respect to gaseous and aqueous chemistry, the effect of water flow rate was found negligible (data not shown), as long as the ratio of the total water volume and water treatment time was kept constant.

Besides concentrations of H_2O_2, NO_2^- and NO_3^- in water, we also evaluated the relative concentration of ·OH radical in water solution as a function of N_2/O_2 ratio. For ·OH analysis an aqueous solution of TA and NaOH was used, as described in section "Water Analysis". Due to the fact that TA may not be fully specific for ·OH detection in plasma treated liquids (as we explained in section "Water Analysis") the relative concentration of ·OH radicals is presented as HTA fluorescence (Fig. 7). The ·OH radical profile as a function of N_2/O_2 ratio qualitatively correlates with the H_2O_2 profile, which supports the idea of ·OH involvement in the H_2O_2 production. The relative ·OH radical concentration increased with the increasing O_2 concentration in gas mixture and in pure O_2 it was almost one order of magnitude higher when compared to pure N_2. Considering the optimal case of the maximum possible reaction efficiency of OH radicals with TA and assuming a good specificity of their reaction with TA, the maximum absolute concentration of ·OH radicals in N_2/O_2 mixtures would be 0.04 mM. However, the real OH concentration is most probably much smaller than this. Decreasing water treatment time from 10 to 5 min (both per 5 mL) led to a decrease of ·OH relative concentration to approximately half value (data not shown).

The plasma induced chemistry is strongly dependent on pH of the treated water solution. The problem with ·OH measurements with TA is that prior to the plasma activation, pH of the solution had to be significantly increased to basic values by NaOH to enable TA solvation. Due to this increased pH values with respect to the typical PAW, we can
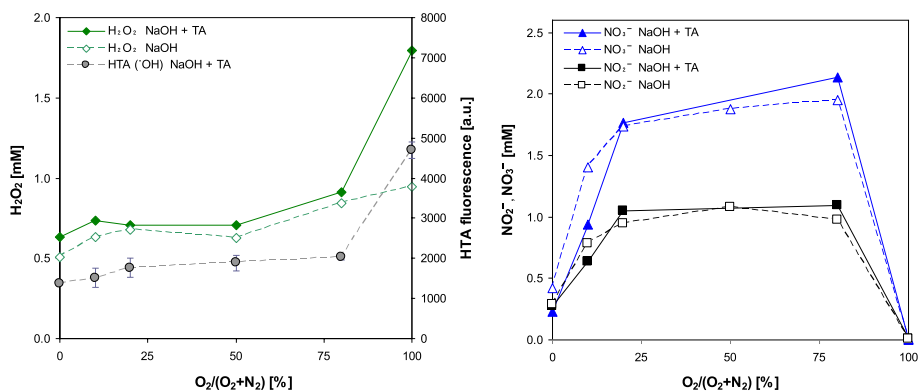
Fig. 7 Concentrations of NO_2^-, NO_3^- in NaOH solution and concentration of H_2O_2, and ·OH radical (HTA fluorescence) in NaOH + TA (·OH radical probe) solution as a function of gas mixture (N_2/O_2 ratio) [gas flow rate Q = 0.5 L/min, water treatment time 10 min]

expect different chemical reactions in these alkaline solutions (NaOH or NaOH + TA, initial pH 11.5 and 10, respectively) used for $^.OH$ radical measurement than in water (initial pH 5) used for H_2O_2, NO_2^- and NO_3^- measurements. To be able to relate the concentration of $^.OH$ radicals with other species, we measured the pH and concentration of H_2O_2, NO_2^- and NO_3^- not only in PAW, but also in water solutions with NaOH + TA and with NaOH. Figure 7 shows concentrations of $^.OH$ and H_2O_2 in NaOH + TA solution ($^.OH$ radical probe) and concentrations of NO_2^-, NO_3^- in NaOH solution as a function of gas mixture (N_2/O_2 ratio). As the figure shows, the concentrations of NO_2^- and NO_3^- in NaOH solution have similar profiles as in PAW (Fig. 6), despite different initial pH. H_2O_2 concentration was lower in water in the mixtures at 20–80% O_2 in N_2 than in NaOH + TA solution, which might be attributed to H_2O_2 depletion by the reaction with NO_2^- in acidic conditions (previously mentioned peroxynitrite mechanism) that does not occur here in basic environment. No occurrence of the peroxynitrite mechanism, which depletes H_2O_2 in acidic conditions, here in the basic environment of NaOH (and NaOH + TA), is probably also responsible for the relatively flat H_2O_2 (and $^.OH$) profiles across 0–80% O_2 in N_2, since it was mainly NO_2^- that was sensitive to N_2/O_2 ratio in PAW and this NO_2^- depleted H_2O_2 in PAW. The increase of H_2O_2 and $^.OH$ in pure O_2 is discussed later. Besides other reactions in PAW, the decrease of pH in NaOH + TA solution with respect to NaOH only could be assigned to TA hydroxylation ($TA + ^.OH \rightarrow HTA + H^+$).

As [91, 98] reported, the main pathway for the production of H_2O_2 is 3-body recombination of $^.OH$ radicals in the gas. According to several more research papers [23, 51, 52], H_2O_2 is dominantly produced in the gas phase and then easily dissolves in water, since its Henry's law solubility is very high [85]. Therefore, one may presume that the presence of TA and NaOH in the water, as well as the increased pH, should not affect the chemistry in the gas and perhaps neither the H_2O_2 transport into water. Kurake et al. [99] found no notable changes in H_2O_2 concentration in the PAW with D-mannitol used as $^.OH$ radical probe. They suggested that in their case H_2O_2 could be formed via the pathway of water dissociation to molecular H_2 and O_2 ($2H_2O \rightarrow 2H_2 + O_2 \rightarrow H_2 + H_2O_2$), as it was previously suggested by Jablonowski et al. [100]. Interestingly, we measured a higher concentration of H_2O_2 in NaOH + TA than in the NaOH treated in pure O_2 plasma. This phenomenon can be explained by the fact that in pure O_2, in an excess of $^.OH$, besides H_2O_2 formation, $^.OH$ may also contribute to the H_2O_2 decomposition (while producing $HO_2^.$) [81, 93]. However, in the presence of the $^.OH$ scavenging probe, the H_2O_2 decomposition by $^.OH$ might be suppressed, as reported by [84]. On the other hand, and in agreement with our results, higher H_2O_2 concentration in the solution with $^.OH$ probe in pure O_2 was also reported by Honnorat et al. [101]. We should note that the intermediate product of Peroxone process (reaction of H_2O_2 with O_3) taking place in the basic solution with $^.OH$ probe is $HO_2^.$ and the final product is $^.OH$ [93]. $^.OH$ could recombine with another $^.OH$ to reproduce H_2O_2 and contribute to the H_2O_2 surplus in NaOH + TA solution treated in pure O_2 atmosphere.

H_2O_2 decay can be also possibly caused by O atoms in addition to O_3 via Peroxone process mentioned above. O atoms are largely produced by TS plasma in the gas phase and can be dissolved into the liquid [52, 93]. In the presence of TA ($^.OH$ radical probe), O atoms are also scavenged by TA (the problem of selectivity of TA was discussed in section "Water Analysis"). The scavenged O atoms cannot react with H_2O_2 directly and cannot form O_3 (3-body reaction with O_2 described in section "Chemical Species in Gas Mixtures without Water Flow"), which would also keep higher H_2O_2 concentration. So, the TA, besides scavenging $^.OH$, scavenges also other species (e.g. O) that would normally reduce the amounts of H_2O_2, and therefore we detected a surplus of H_2O_2. The similarity in $^.OH$

with H_2O_2 profiles (Fig. 7) indicate a certain correlation, however these results should be verified with another ·OH probe (e.g. DMSO) in future.

Antibacterial Effects

The chemical analyses of the gas mixtures and water were correlated to the antibacterial effect of TS discharge on *Escherichia coli* in water. The decrease of bacterial population was observed for all of three N_2/O_2 gas mixtures (pure O_2 gas, air-like mixture (20% O_2 in N_2) and in pure N_2). Figure 8 shows the log reduction of *E. coli* as a function of the gas mixture (N_2/O_2 ratio) and also as a function of the gas flow rate Q and water treatment time. The best antibacterial effects were observed in the mixtures where both N_2 and O_2 were present. The maximum 3.6 ± 0.3 logs was found at 20% O_2 in N_2 with the gas flow rate Q = 0.5 L/min and 10 min water treatment time. These results for Q = 0.5 L/min and 10 min are shown together with a faster gas flow rate 2 L/min and shorter water treatment time 5 min. Faster gas flow rate resulted in lower gaseous RONS concentrations (Fig. 3) as a result of shorter residence time and smaller discharge energy delivered to the same gas volume. Consequently, higher aqueous RONS concentrations were detected with the slower Q, thus we observed a stronger antibacterial effect. Similarly, longer water treatment time (10 min as opposed to 5 min) also expectedly resulted in stronger antibacterial effect. Both parameters (slower Q and longer water treatment time) play together and resulted in a stronger antibacterial effect.

The pH decrease probably plays a crucial role as it increases the reactivity of radicals [44]. The low acidic pH accelerates the reaction between H_2O_2 and NO_2^- to form ONOOH and subsequently radicals are rapidly produced without giving bacteria enough chances to respond with their innate antioxidant systems.

We observed a slightly higher *E. coli* inactivation here in the closed reactor with air (20% O_2 in N_2) flow of 0.5 L/min (~ 3.6 logs) than in the open reactor in ambient air (~ 3.2 logs) with the same water treatment time 10 min [102]. The result can be attributed to a higher humidity and subsequent higher ·OH radical production in the closed reactor. The dependence of ·OH radical concentration on the gas humidity was also investigated by Winter et al. [98]. They also found higher concentrations of RONS in PAW produced in the closed reactor than in the open reactor.

In pure N_2 we measured a significant inactivation of *E. coli* ~ 2.1 to 2.7 log, despite only traces of NO_x in the gas and only low concentrations of NO_2^- and NO_3^- in the water were detected. The inactivation is unlikely to be attributed to the UV radiation, as it is probably

Fig. 8 Inactivation of *E. coli* in water as a function of the gas mixture (N_2/O_2 ratio), gas flow rate Q = 2 and 0.5 L/min and water treatment time 5 and 10 min
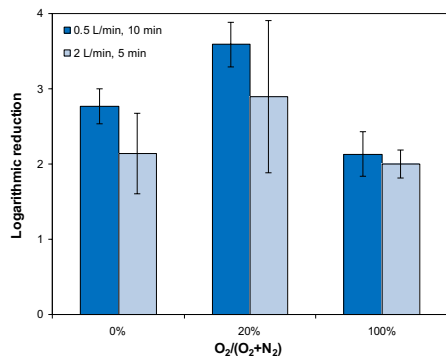
not important in our experimental conditions [37]. Neither increased temperature could cause the bacterial inactivation, as *E. coli* showed no vulnerability during a short high temperature test (10 min, 60 °C). As the bacteria are suspended in the solution flowing directly through the discharge, the contribution from the pulsed electric field may be important. Potential production of NH_3 even in very low concentrations in PAW under our detection limit could also contribute to the antibacterial effect, as NH_3 is known to be toxic. Nevertheless, significant H_2O_2 (Fig. 6) and even ˙OH radical concentrations (Fig. 7) in combination with a slight pH decrease and low concentrations of NO_2^- and NO_3^- are the most probable factors of this inactivation. This issue needs, however, further investigations.

In pure O_2 where pH did not decrease and NO_2^- and NO_3^- were absent in plasma treated water, the key antibacterial species ONOOH could not be produced. Despite the lack of reactive nitrogen species, we still observed an inactivation of *E. coli* ~2–2.1 log. Similar to pure N_2, factors like UV or elevated temperature can be excluded, however not the effect of the pulsed electric field. On the other hand, in pure O_2 atmosphere, O_3 can be partly responsible for bacterial inactivation, as it has a well-know antibacterial capability [103] and was the only species detected by FTIR. However, as we mentioned previously, we did not detect O_3 in the TS treated water. Therefore, we assume the high concentration of H_2O_2 and especially ˙OH could possibly play a more important role in bacterial inactivation in pure O_2 atmosphere. The potential role of plasma-generated atomic O that transfers into water must be analyzed in greater depth in future investigations.

Conclusions

The objective of this study was to investigate the effect of gas composition (N_2/O_2 ratio) on the production of RONS in gas and in water by transient spark discharge and their subsequent effects on bacteria. The effects of transient spark discharge have been previously studied in the system with water electrospray and in air mixtures. This study has been performed in the system with water flowing down the inclined grounded electrode and in various gas mixtures: 0, 10, 20, 50, 80, and 100% of O_2 in N_2. The gas flow rate was controlled in the range of 0.25–2.2 L/min and water treatment times 5 and 10 min. The concentrations of various species in the gas phase (NO_x, N_2O, HNO_2, O_3) and in water (˙OH, H_2O_2, NO_2^-, NO_3^-) were measured as functions of gas mixture composition, gas flow rate and water treatment time. Besides the chemical analysis, the effect on *E. coli* was investigated to understand the plasma components responsible for antibacterial effects.

The transient spark discharge of positive polarity was used, with average discharge power P ~ 4.5–7 W depending on the gas mixture composition, i.e. N_2/O_2 ratio and the presence of water that affected the overall discharge stability. The chemical analysis of the gas has detected NO and NO_2 as the dominant gaseous species. The NO and NO_2 concentrations increased with O_2 up to 50%, reached a maximum 764 ppm and 302 ppm, respectively (at 0.5 L/min gas flow rate), and then decreased with the further increase of O_2. The concentration of NO was higher than NO_2 as it is a primary product of Zeldovich mechanism. NO and NO_2 concentrations decreased with the increasing gas flow rate, as a result of shorter residence time of gas mixture in the discharge zone. In mixtures without water, small concentration of N_2O was detected (up to 3.5 ppm), especially with low O_2 concentration (below 5% O_2 in N_2). With respect to its low concentration the effect of N_2O to the overall chemistry was considered negligible. On the other hand, in the mixtures with high O_2 concentrations (in pure O_2), O_3 production was detected (up to 207 ppm). Its

concentration became negligible with the increase of N_2, as a result of high gas temperature and formation of NO_x.

When water flowed down the grounded electrode, the reaction mechanisms changed and species such as $^{.}OH$ and H_2O_2 were generated as a result of H_2O dissociation and subsequent recombination. With water, NO can be easily oxidized to NO_2, while $^{.}OH$ radicals are also essential for further oxidation of NO_x to nitrogen acids HNO_x. With water we observed similar profile of NO and NO_2 concentrations in dependence on N_2/O_2 ratio as in the system without water, although the absolute NO_x concentrations were lower. The reason is oxidation of NO and NO_2 to HNO_2 or HNO_3, as well as direct dissolution of NO and NO_2 into water. HNO_2 was also detected among the gaseous products. With the increasing gas flow rate the concentrations of all gaseous species decreased. Besides NO, NO_2 and HNO_2, no other nitrogen species were detected in the FTIR spectra. O_3 was detected only in pure O_2, but in smaller concentration (125 ppm) compared to the case without water. O_3 rapidly decays in a reaction with NO, $^{.}OH$, and also partially due to its dissolution in water. On the other extend, in pure N_2 with water, small concentrations of NO, NO_2 and HNO_2 were formed, since the source of O and $^{.}OH$ necessary for NO_x formation was probably the H_2O dissociation, while without water none of them was detected. As the concentration of individual species produced in the gas phase was often strongly affected and determined by their solvation in water depending on their Henry's law solubility constants, we also measured and evaluated the concentration of selected reactive species in PAW.

The analyzed reactive species in water were H_2O_2, NO_3^-, NO_2^- and $^{.}OH$. H_2O_2 was produced mostly in the gas phase by recombination of $^{.}OH$ radicals and subsequently dissolved into water. Nitrites NO_2^- and nitrates NO_3^- are mainly the result of gaseous NO and NO_2 and gaseous HNO_2 and HNO_3 dissolved in water, resulting in acidification of PAW. In pure N_2, considerable concentrations of all RONS species were found and their concentration was governed by the dissociation of H_2O leading to the formation of $^{.}OH$ (0.03 mM), H_2O_2 (0.9 mM), NO_2^- (0.4 mM) and NO_3^- (0.7 mM), and significant pH decrease (from 5 to 3.5). At the other extreme, in pure O_2 the highest concentrations of $^{.}OH$ (0.2 mM) and H_2O_2 (1.8 mM) were detected in water, however no O_3, NO_2^- or NO_3^- and a minimal pH decrease (from 5 to 4.3). H_2O_2 accumulated in PAW in O_2, due to the lack of NO_2^- it could potentially react with. Although O_3 is a dominant gaseous product in pure O_2, it was not detected in water, neither applies the Peroxone process leading to additional $^{.}OH$ radical formation. In mixtures containing both O_2 and N_2, the concentration of H_2O_2 (0.4 mM) and $^{.}OH$, as well as pH (2.9) decreased to their minima, while concentrations of NO_2^- (0.7 mM) and NO_3^- (4.0 mM) increased and reached the maximum at 50% O_2 in N_2. The profile of H_2O_2 concentration as a function of N_2/O_2 ratio is similar to the profile of $^{.}OH$ radicals, which supports the idea of $^{.}OH$ involvement in the H_2O_2 production. Besides N_2/O_2 ratio, the effects of gas and water flow rates on gaseous and aqueous chemistry was investigated, too. The effect of gas flow rate was found significant, but the effect of water flow rate was found negligible with the constant water treatment time. By increasing the gas flow rate from 0.25 to 2 L/min, H_2O_2 concentration increased and NO_2^- concentration decreased, due to decreased NO_x gaseous concentrations as a result of shorter residence time and NO_2^- depletion in the reaction with H_2O_2 leading to peroxynitrites.

Chemical analysis of gas and water were correlated with the antibacterial effect of TS plasma on *E. coli* in water suspension. The best antibacterial effects were found in the mixtures with both N_2 and O_2 present. The maximum bacterial inactivation (~3.6 logs) was found at 20% O_2 in N_2 with 0.5 L/min gas flow rate and 10 min water treatment time. It can be explained by the synergic effect of H_2O_2 and NO_2^- in acidic PAW, which leads to the production of $ONOO^-/ONOOH$ at acidic pH, as a result of accelerated reaction of H_2O_2

and NO_2^-. These RONS play an important role in antibacterial activity of PAW, as they may cause cell membrane peroxidation, especially at acidic pH. In pure N_2 and pure O_2, the bacterial inactivations were lower, 2.5 and 2.0 logs, respectively, most probably being the result of significant H_2O_2 and $^.OH$ concentrations, with minimum contribution from NO_x^-. Finally, the closed reactor with air flow showed stronger inactivation than the open reactor in ambient air, which was attributed to higher $^.OH$ radical production in the closed reactor.

In summary we showed that plasma induced chemistry in the N_2/O_2 gas, in the water and the plasma–liquid interface is essential for understanding of the bacterial inactivation. We demonstrated that the composition of the gas mixture needs to be controlled as it has a significant effect on the bacterial inactivation due to its effects on RONS production and associated chemistry in water.

References

1. Kovaľová Z, Leroy M, Jacobs C, Kirkpatrick M, Machala Z, Lopes F, Laux CO, DuBow M, Odic E (2015) Atmospheric pressure argon surface discharge propagated in long tubes: physical characterization and application to bio-decontamination. J Phys D Appl Phys 48:464003
2. Kovaľová Z, Leroy M, Kirkpatrick M, Odic E, Machala Z (2016) Corona discharges with water electrospray for *Escherichia coli* biofilm eradication on a surface. Bioelectrochemistry 112:91–99
3. Pankaj SK, Bueno-Ferrer C, Misra NN, Milosavljević V, O'Donell CP, Bourke P, Keener KM, Cullen PJ (2014) Applications of cold plasma technology in food packaging. Trends Food Sci Technol 35:5–17
4. Thirumdas R, Sarangapani C, Annapure US (2015) Cold plama: a novel non-thermal technology for food processing. Food Biophys 10:1–11
5. Misra NN, Schülter OK, Cullen PJ (2016) Cold plasma in food and agriculture. Academic Press, Elsevier, London
6. Zahoranová A, Henselová M, Hudecová D, Kaliňáková B, Kováčik D, Medvecká V, Černák M (2016) Effect of cold atmospheric pressure plasma on the wheat seedlings vigor and on the inactivation of microorganisms on the seeds surface. Plasma Chem Plasma Process 36:397–414
7. Puač N, Škoro N, Spasić K, Živković S, Milutinović M, Petrović ZL (2018) Activity of catalase enzyme in Paulownia tomentosa seeds during the process of germination after treatments with low pressure plasma and plasma activated water. Plasma Process Polym 15:1700082
8. Pawlat J, Starek A, Sujak A, Terebun P, Kwiatkowski M, Budzen M, Andrejko D (2018) Effects of atmospheric pressure plasma jet operating with DBD on *Lavatera thuringiaca* L. seed's germination. PLoS ONE 13:0194349
9. Arora V, Nikhil V, Suri NK, Arora P (2014) Cold atmospheric plasma (CAP) in dentistry. Dentistry 4:1000189
10. Gherardi M, Tonini R, Colombo V (2018) Plasma in dentistry: brief history and current status. Trends Biotechnol 36:583–585
11. Bekeschus S, Schmidt A, Weltmann K-D, von Woedtke Th (2016) The plasma jet kINPen—a powerful tool for wound healing. Clin Plasma Med 4:19–28
12. Schmidt A, Bekeschus S, Wende K, Vollmar B, von Woedtke Th (2017) A cold plasma jet accelerated wound healing in a murine model of full-thickness skin wounds. Exp Dermatol 26:156–162
13. Hasse S, Doung Tran T, Hahn O, Kindler S, Metelmann H-R, von Woedtke Th, Masur K (2016) Introduction of proliferation of basal epidermal keratinocytes by cold atmospheric pressure plasma. Clin Exp Dermatol 41:202–209
14. Graves DB (2012) The emerging role of reactive oxygen and nitrogen species in redox biology and some implications for plasma applications to medicine and biology. J Phys D Appl Phys 45:263001
15. Babington P (2015) Use of cold atmospheric plasma in the treatment of cancer. Biointerphases 10:029403

16. Van Boxem W, Van der Paal J, Gorbanev Y, Vanuytsel S, Smits E, Dewilde S, Bogaerts A (2017) Anti-cancer capacity of plasma treated PBS: effect of chemical composition on cancer cell cytotoxicity. Sci Rep 7:16478

17. Yan D, Sherman JH, Keidar M (2017) Cold atmospheric plasma, a novel promising anti-cancer treatment modality. Oncotarget 8:15977–15995

18. Metelmann H-R, Seebauer Ch, Miller V, Fridman A, Bauer G, Graves DB, Pouvesle J-M, Rutkowski R, Schuster M, Bekeschus S, Wende K, Masur K, Hasse S, Gerling T, Hori M, Tanaka H, Choi EH, Weltman K-D, Metelmann PH, Von Hoff DD, von Woedtke Th (2018) Clinical experience with cold plasma in the treatment of locally advanced head and neck cancer. Clin Plasma Med 9:6–13

19. Tornin J, Mateu-Sanz M, Rodríguez A, Labay C, Rodríguez R, Canal C (2019) Pyruvate plays a main role in the antitumoral selectivity of cold atmospheric plasma in osteosarcoma. Sci Rep 9:10681

20. Bauer G, Sersenová D, Graves DB, Machala Z (2019) Cold atmospheric plasma and plasma-activated medium trigger RONS-based tumor cell apoptosis. Sci Rep 9:14210

21. Lukeš P, Doležalová E, Sisrová I, Clupek M (2014) Aqueous-phase chemistry and bactericidal effects from an air discharge plasma in contact with water: evidence for the formation of peroxynitrite through a pseudo-second-order post-discharge reaction of H_2O_2 and HNO_2. Plasma Sources Sci Technol 23:015019

22. Machala Z, Tarabová B, Sersenová D, Janda M, Hensel K (2019) Chemical and antibacterial effects of plasma activated water: correlation with gaseous and aqueous reactive oxygen and nitrogen species, plasma sources and air flow conditions. J Phys D Appl Phys 52:032002

23. Bruggeman PJ, Kushner MJ, Locke BR et al (2016) Plasma-liquid interactions: a review and roadmap. Plasma Sources Sci Technol 25:053002

24. Kruszelnicki J, Lietz AM, Kushner MJ (2019) Atmospheric pressure plasma activation of water droplets. J Phys D Appl Phys 52:355207

25. Heirman P, Van Boxem W, Bogaerts A (2019) Reactivity and stability of plasma-generated oxygen and nitrogen species in buffered water solution: a computational study. Phys Chem Chem Phys 21:12881–12894

26. Lu P, Boehm D, Bourke P, Cullen PJ (2017) Achieving reactive species specificity within plasma-activated water through selective generation using air spark and glow discharges. Plasma Process Polym 14:1600207

27. Niquet R, Boehm D, Schnabel U, Cullen P, Bourke P, Ehlbeck J (2018) Characterising the impact of post-treatment storage on chemistry and antimicrobial properties of plasma treated water derived from microwave and DBD sources. Plasma Process Polym 15:1700127

28. Khlyustova A, Labay C, Machala Z, Ginebra MP, Canal C (2019) Important parameters in plasma jets for the production of RONS in liquids for plasma medicine: a brief review. Front Chem Sci Eng 13:238–252

29. Pawlat J, Terebun P, Kwiatkowski M, Tarabová B, Kovaľová Z, Kučerová K, Machala Z, Janda M, Hensel K (2019) Evaluation of oxidative species in gaseous and liquid phase generated by mini-gliding arc discharge. Plasma Chem Plasma Process 39:627–643

30. Tresp H, Hammer MU, Winter J, Weltmann K-D, Reuter S (2013) Quantitative detection of plasma-generated radicals in liquids by electron paramagnetic resonance spectroscopy. J Phys D Appl Phys 46:435401

31. Jablonowski H, Hänsch MACh, Dünnbier M, Wende K, Hammer MU, Weltman K-D, Reuter S, von Woedtke Th (2015) Plasma jet's shielding gas impact on bacterial inactivation. Biointerphases 10:029506

32. von Woedtke Th, Metelmann H-R, Weltmann K-D (2014) Clinical plasma medicine: state and perspectives of in vivo application of cold atmospheric plasma. Contrib Plasma Phys 54:104–117

33. Isbary G, Shimizu T, Zimmermann JL, Heinlin J, Al-Zaabi S, Rechfeld M, Morfill GE, Karrer S, Stolz W (2014) Randomized placebo-controlled clinical trial showed cold atmospheric argon plasma relieved acute pain and accelerated healing in herpes zoster. Clin Plasma Med 2:50–55

34. Girard F, Peret M, Dumont N, Badets V, Blanc S, Gazeli K, Noël C, Belmonde T, Marlin L, Cambus J-P, Simon G, Sojic N, Held B, Arbaut S, Clément F (2018) Correlation between gaseous and liquid phase chemistries induced by cold atmospheric plasmas in a physiological buffer. Phys Chem Chem Phys 20:9198–9210

35. Uchida G, Nakajima A, Ito T, Takenaka K, Kawasaki T, Koga K, Shiratani M, Setsuhara Y (2016) Effects of nonthermal plasma jet irradiation on the selective production of H_2O_2 and NO_2^- in liquid water. J Appl Phys 120:203302

36. Ito T, Uchida G, Nakajima A, Takenaka K, Setsuhara Y (2017) Control of reactive oxygen and nitrogen species production in liquid by nonthermal plasma jet with controlled surrounding gas. Jpn J Appl Phys 56:01AC06

37. Machala Z, Tarabová B, Hensel K, Špetlíková E, Šikurová L, Lukeš P (2013) Formation of ROS and RNS in Water Electro-Sprayed through Transient Spark Discharge in Air and their Bactericidal Effects. Plasma Process Polym 10:649–659

38. Graves DB (2014) Reactive species from cold atmospheric plasma: implications for cancer therapy. Plasma Process Polym 11:1120–1127

39. Girard F, Badets V, Blanc S, Gazeli K, Marlin L, Authier L, Svarnas P, Sojic N, Clement P, Arbault S (2016) Formation of reactive nitrogen species including peroxynitrite in physiological buffer exposed to cold atmospheric plasma. RSC Adv 6:78457–78467

40. Kono Y, Shibata H, Adachi K, Tanaka K (1994) Lactate-dependent killing of *Escheriachia coli* by nitrite plus hydrogen peroxide: a possible role of nitrogen dioxide. Arch Biochem Biophys 311:153–159

41. Ke Z, Thopan P, Fridman G, Miller V, Yu L, Fridman A, Huang Q (2017) Effect of N_2/O_2 composition on inactivation efficiency of *Escherichia coli* by discharge plasma at the gas-solution interface. Clin Plasma Med 7–8:1–8

42. Satoh K, Scott J, MacGregor J, Anderson JG (2007) Pulsed-plasma disinfection of water containing *Escherichia coli*. Jpn J Appl Phys 46:1137–1141

43. Oehmigen K, Hähnel M, Brandenburg R, Wilke Ch, Weltmann K-D, von Woedtke T (2010) The role of acidification for antimicrobial activity of atmospheric pressure plasma in liquids. Plasma Process Polym 7:250–257

44. Liu Z, Xu D, Liu D, Cui Q, Cai H, Li Q, Chen H, Kong MG (2017) Production of simplex RNS and ROS by nanosecond pulse N_2/O_2 plasma jets with homogenous shielding gas for inducing myeloma cell apoptosis. J Phys D Appl Phys 50:195204

45. Hozák P, Scholtz V, Khun J, Mertová D, Vaňková E, Julák J (2018) Further contribution to the chemistry of plasma-activated water: influence on bacteria in planktonic and biofilm forms. Plasma Phys Rep 44:799–804

46. Julák J, Hujacová A, Scholtz V, Khun J, Holada K (2018) Contribution to the chemistry of plasma-activated water. Plasma Phys Rep 44:125–136

47. Qi Z, Tian E, Song Y, Sosnin EA, Skakun VS, Li T, Xia Y, Zhao Y, Lin XS, Liu D (2018) Inactivation of *Shewanella putrefaciens* by plasma activated water. Plasma Chem Plasma Process 38:1035–1050

48. Kondeti VSSK, Phan CQ, Wende K, Jablonowski H, Gangal U, Granick JL, Hunter RC, Bruggeman PJ (2018) Long/lived and short/lived reactive species produced by a cold atmospheric pressure plasma jet for the inactivation of *Pseudomonas aeruginosa* and *Staphylococcus aureus*. Free Radic Biol Med 124:275–287

49. Anderson CE, Cha NR, Lindsay AD, Clark DS, Graves DB (2016) The role of interfacial reactions in determining plasma/liquid chemistry. Plasma Chem Plasma Process 36:1393–1415

50. Zhang Z, Xu Z, Cheng Ch, Wei J, Lan Y, Ni G, Sun Q, Qian S, Zhang H, Xia W, Shen J, Meng Y, Chu PK (2017) Bactericidal effects of plasma induced reactive species in dielectric barrier gas-liquid discharge. Plasma Chem Plasma Process 37:415–431

51. Hefny MM, Pattyn C, Lukeš P, Benedikt J (2016) Atmospheric plasma generates oxygen atoms as oxidizing species in aqueous solutions. J Phys D Appl Phys 49:404002

52. Benedikt J, Hefny MM, Shaw A, Buckley BR, Iza F, Schäkermann S, Bandow JE (2018) The fate of plasma-generated oxygen atoms in aqueous solutions: non-equilibrium atmospheric pressure plasmas as an efficient source of atomic O(aq). Phys Chem Chem Phys 20:12037

53. Ikawa S, Tani S, Nakashima Y, Kitano K (2016) Physicochemical properties of bactericidal plasma-treated water. J Phys D Appl Phys 49:425401

54. Shaw P, Kumar N, Kwak HS, Park HJ, Uhm HS, Bogaerts A, Choi EH, Attri P (2018) Bacterial inactivation by plasma treated water enhanced by reactive nitrogen species. Sci Reports 8:11268

55. Chen TP, Liang J, Su TL (2018) Plasma-activated water: antibacterial activity and artifacts? Environ Sci Pollut Restor 27:26699–26706

56. Eto H, Ono Y, Ogino A, Nagatsu M (2008) Low-temperature sterilization of wrapped materials using flexible sheet-type dielectric barrier discharge. Appl Phys Lett 93:221502

57. van Bokhorst-van de Veen H, Xie H, Esveld E, Abee T, Mastwijk H, Groot MN (2015) Inactivation of chemical and heat-resistant spores of Bacillus and Geobacillus by nitrogen cold atmospheric plasma evoked distinct changes in morphology and integrity of spores. Food Microbiol 45:26–33

58. Abonti TR, Kaku M, Kojima S, Sumi H, Kojima S, Yamamoto T, Yashima Y, Miyahara H, Okino A, Kawata T, Tanne K, Tanimoto K (2016) Irradiation effects of low temperature multigas plasma jet on oral bacteria. Dent Mater J 35:822–828

59. Machala Z, Janda M, Hensel K, Jedlovský I, Leštinská L, Foltin V, Martišovitš V, Morvová M (2007) Emission spectroscopy of atmospheric pressure plasmas for bio-medical and environmental applications. J Mol Spectrosc 243:194–201

60. Janda M, Martišovitš V, Machala Z (2011) Transient spark: a dc-driven repetitively pulsed discharge and its control by electric circuit parameters. Plasma Sci Technol 20:035015
61. Janda M, Machala Z, Niklová A, Martišovitš V (2012) The streamer-to-spark transition in a transient spark: a dc-driven nanosecond-pulsed discharge in atmospheric air. Plasma Sources Sci Technol 21:045006
62. Janda M, Martišovitš V, Hensel K, Machala Z (2016) Generation of antimicrobial NOx by atmospheric air transient spark dsicharge. Plasma Chem Plasma Process 36:767–781
63. Eisenberg GM (1943) Colorimetric determination of hydrogen peroxide. Ind Eng Chem 15:327–328
64. Griess P (1879) Bemerkungen zu der Abhandlung der HH. Weselsky und Benedikt "Ueber einige Azoverbindungen". Ber Dtsch Chem Ges 12:426–428
65. Moorcroft MJ, Davis J, Compton RG (2001) Detection and determination of nitrate and nitrite: a review. Talanta 54:785–803
66. Tarabová B, Lukeš P, Janda M, Hensel K, Šikurová L, Machala Z (2018) Specificity of detection methods of nitrites and ozone in aqueous solutions activated by air plasma. Plasma Process Polym 15:e1800030
67. Charbouillot T, Brigane M, Mailhot G, Maddigapu PR, Minero C, Vione D (2011) Performance and selectivity of the terephthalic acid probe for ˙OH as function of temperature, pH and composition of atmospherically relevant aqueous media. J Photochem Photobiol A 222:70–76
68. Saran M, Summer KH (1999) Assaying for hydroxyl radicals: hydroxylated terephthalate is a superior fluorescence marker than hydroxylated benzoate. Free Rad Res 31:429–436
69. Kanazawa S, Furuki T, Nakaji T, Akamine S, Ichiki R (2013) Application of chemical dosimetry to hydroxyl radical measurement during underwater discharge. J Phys Conf Ser 418:012102
70. Mark G, Tauber A, Laupert R, Schuchmann H-P, Schultz D, Mues A, von Sonntag C (1998) OH-radical formation by ultrasound in aqueous solution-Part II: terephthalate and Fricke dosimetry and the influence of various constrictions on the sonolytic yield. Ultrasound Chem 5:41–42
71. Miller JA, Bowman CT (1989) Mechanism and modeling of nitrogen chemistry in combustion. Prog Energy Combust Sci 15:287–338
72. Kossyi IA, Kostinsky AYu, Matveyev AA, Silakov VP (1992) Kinetic scheme of non-equilibrium discharge in N_2-O_2 mixtures. Plasma Source Sci Technol 1:207–220
73. Lowke JJ, Morrow R (1995) Theoretical analysis of removal of oxides of sulphur and nitrogen in pulsed operation of electrostatic precipitators. IEEE Trans Plasma Sci 23:661–671
74. Fan X, Kang S, Li J, Zhu T (2018) Formation of nitrogen oxides (N_2O, NO, and NO_2) in typical plasma and plasma-catalytic processes for air pollution control. Water Air Soil Pollut 229:351
75. Krawczyk K, Mlotek M (2001) Combined plasma-catalytic processing of nitrous oxide. Appl Catal B 30:233–245
76. Morgan MM, Cuddly MF, Fisher ER (2010) Gas-phase chemistry in inductively coupled plasmas for NO removal from mixed gas systems. J Phys Chem 114:1722–1733
77. Dahiya RP, Mishra SK, Veefkind A (1993) Plasma chemical investigation for NOx and SO_2 removal from flue gases. IEEE Trans Plasma Sci 21:346–348
78. Smith IWM, Tuckett RP, Whitham CJ (1993) Vibrational state specificity and selectivity in the reactions $N + OH \rightarrow NO(v) + H$ and $N + NO(v) \rightarrow N_2 + O$. J Chem Phys 98:6267–6275
79. Lukeš P, Locke BR, Brisset JL (2012) In: Parvulescu VI, Magureanu M, Lukeš P (eds) Elementary chemical and physical phenomena in electrical discharge plasma in gas-liquid environments and in liquids. Plasma chemistry and catalysis in gases and liquids, 1st edn. Wiley-VCH Verlag GmbH & Co. KGaA, Weinheim
80. Sridharan UC, Reimann B, Kaufman F (1980) Kinetics of the reaction $OH + H_2O_2 \rightarrow HO_2 + H_2O$. J Chem Phys 73:1286–1293
81. Christensen H, Sehested K, Corfitzen H (1982) Reactions of hydroxyl radicals with hydrogen peroxide at ambient and elevated temperature. J Phys Chem 86:1588–1590
82. Anderson G, Kaufman F (1973) Kinetics of the reaction $OH (v = 0) + O_3 \rightarrow HO_2 + O_2$. Chem Phys Lett 19:483
83. Kuhl AL, Leyer J-C, Sirignano WA, Borisov AA (1993) Dynamics of gaseous combustion. Aerospace Research Central, AIAA, Reston
84. Kovačević VV, Dojcinovic BP, Jovic M, Roglic GM, Obradovic BM, Kuraica MM (2017) Measurement of reactive species generated by dielectric barrier discharge in direct contact with water in different atmospheres. J Phys D Appl Phys 50:155205
85. Sander R (2015) Compilation of Henry's law constants (version 4.0) for water as solvent. Atmos Chem Phys 15:4399–4981
86. Fridman A (2008) Plasma chemistry. Cambridge University Press, Cambridge

87. Bader H, Hoigné J (1981) Determination of ozone in water by the indigo method. Water Res 15:449–456
88. Sasakura T, Uemura S, Hino M, Kiyomatsu S, Takatsuji Y, Yamasaki R, Morimoto M, Haruyama T (2018) Excitation of H_2O at the plasma/water interface by UV irradiation for the elevation of ammonia production. Green Chem 20:627–633
89. Haruyama T, Namise T, Shimoshimizu N, Uemura S, Takatsuji Y, Hino M, Yamasaki R, Kamachi T, Kohno M (2016) Non-catalyzed one-step synthesis of ammonia from atmospheric air and water. Green Chem 18:4536–4541
90. Wójtowicz MA, Miknis FP, Grimes RW, Smith WW, Serio MA (2000) Control of nitric oxide, nitrous oxide, ad ammonia emission using microwave plasmas. J Hazard Mater 74:81–89
91. Gorbanev Y, O'Connell D, Chechik V (2016) Non-thermal plasma in contact with water: the origin of species. Chem Eur J 22:1–11
92. Gorbanev Y, Verlackt CCW, Tinck S, Tuenter E, Foubert K, Cos P, Bogaerts A (2018) Combining experimental and modeling approach to study the sources of reactive species induced in water by the COST RF plasma jet. Phys Chem Chem Phys 20:2797–2808
93. Lukeš P, Locke BR, Brisset J-L (2012) In: Parvulescu VI, Magureanu M, Lukeš P (eds) Aquaeous-phase chemistry of electrical discharge plasma in water and in gas-liquid environments. Plasma chemistry and catalysis in gases and liquids, 1st edn. Wiley-VCH Verlag GmbH & Co. KGaA, Weinheim
94. He B, Ma Y, Gong X, Long Z, Li J, Xiong Q, Liu H, Chen Q, Zhang X, Yang S, Liu QH (2017) Simultaneous quantification of aqueous peroxide, nitrate, and nitrite during the plasma-liquid interactions by derivate absorption spectrophotometry. J Phys D Appl Phys 50:445207
95. Brisset J-L, Hnatiuc E (2012) Peroxynitrite: a re-examination of the chemical properties of non/thermal discharges burning in air over aqueous solutions. Plasma Chem Plasma Process 32:655–674
96. Gupta D, Haris B, Kissner R, Koppenol WH (2009) Peroxynitrates is formed rapidly during decomposition of peroxynitrite at neutral pH. Dalton Trans 29:5730–5736
97. Li Y, Sella C, Lemaitre F, Guille-Collignon M, Thouin L (2014) Electrochemical detection of nitric oxide and peroxynitrite anion in microchannels at highly sensitive platinum-black coated electrodes. application to ROS and RNS mixtures prior to biological investigations. Electrochim Acta 144:111–118
98. Winter J, Tresp H, Hammer MU, Iseni S, Kupsch S, Schmidt-Bleker A, Wende K, Dünnbier M, Masur K, Weltmann K-D, Reuter S (2014) Tracking plasma generated H_2O_2 from gas into liquid phase and revealing its dominant impact on human skin cells. J Phys D Appl Phys 47:285401
99. Kurake N, Tanaka H, Ishikawa K, Takeda K, Hashizume H, Nakamura K, Kajiyama H, Kondo T, Kikkawa F, Mizuno M, Hori M (2017) Effects of ˙OH and ˙NO radicals in the aqueous phase on H_2O_2 and NO_2^- generated in plasma-activated medium. J Phys D Appl Phys 50:155202
100. Jablonowski H, Bussiahn R, Hammer MU, Weltmann K-D, von Woedtke Th, Reuter S (2015) Impact of plasma jet vacuum ultraviolet radiation on reactive oxygen species generation in bio-relevant liquids. Phys Plasmas 22:122008
101. Honnorat B, Duchesne C, Liu B, Rousseau A (2018) The scavenging of hydroxyl radical by terephthalic acid and methanol provide insight of ˙OH concentration in liquid phase during plasma-liquid interactions. In: 7th international conference on plasma medicine, Philadelphia, PA, June 17–22, Book of Abstracts, p 230
102. Hensel K, Kučerová K, Tarabová B, Janda M, Machala Z, Sano K, Mihai CT, Gorgan LD, Jijie R, Pohoata V, Topala I (2015) Effects of air transient spark discharge and helium plasma jet on water, bacteria, cells and biomolecules. Biointerphases 10:029515
103. Pavlovich MJ, Chang H-W, Sakiyama Y, Clark DS, Graves DB (2013) Ozone correlates with antibacterial effects from indirect air dielectric barrier discharge treatment of water. J Phys D Appl Phys 46:145202